

PCPDTBT nanostructures and PCPDTBT:PC₇₁BM nanocomposite synthesize via modified polymer-melt technique

Muhamad Doris, Khaulah Sulaiman and Azzuliani Supangat

Abstract

PCPDTBT nanostructures have been synthesized via template-assisted method and polymer-melt technique. The morphological, optical and structural properties of the PCPDTBT have been investigated. Melting polymer was used as a driving force to infiltrate the Anodic Aluminum Oxide (AAO) template in which the applied temperatures are 200, 250, 300, 350, 400 and 450 Celsius respectively. The melting time duration is set constant for 30 minutes for each of those melting temperatures. Nanowires constructions have been produced at all melting temperature however based the morphological investigation, only the first two melting temperatures, 200 and 250, that can serve the structural without any broken noticed on the Raman measurement. The optical and structural properties are also confirm this fact.

Background

Material and methods

The primary element material in this study is a conjugated polymer Poly[2,6-(4,4-bis-(2-ethylhexyl) -4H-cyclopenta [2,1-b;3,4-b'] dithiophene)-alt-4,7(2,1,3-benzothiadiazole)] (PCPDTBT) that was purchased from Sigma-Aldrich, and its chemical structure is shown in Figure 1(a). 5 mg of PCPDTBT was dissolved in 1 ml of chloroform to produce 5 mg/ml concentration of a solution and stirred overnight without any additional purification. To construct a

nanocomposite, a second material, [6,6]-phenyl C₇₁ butyric acid methyl ester (PC₇₁BM), Figure 1(b), was incorporated with PCPDTBT to produce PN-type nanocomposite.

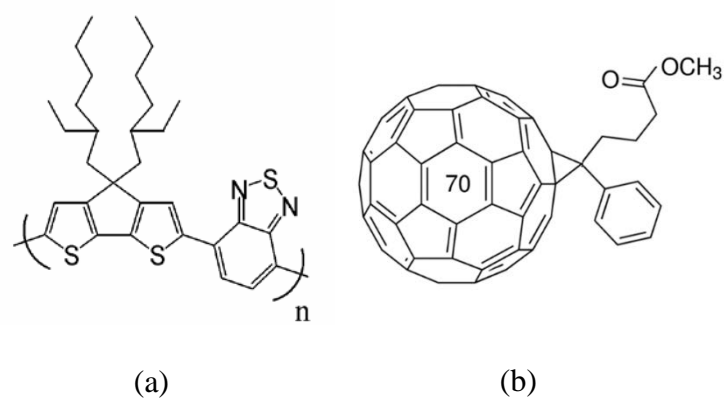


Figure 1 Molecular structure of (a) Donor material, PCPDTBT (Cesare Soci et al., 2006), and (b) Acceptor material, PC₇₁BM.

Inside a furnace chamber, a thick-polymer layer is placed on top of an AAO template nanopores

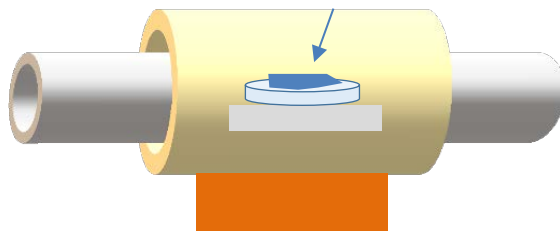


Figure 2: An illustration of the polymer melting process of a thick polymer layer inside a furnace chamber.

Figure 3 reveals an entire illustration of the polymer-melt method to construct the PCPDTBT nanostructures (P-type) and the PCPDTBT:PC₇₁BM nanocomposite (PN-type). The P-type fabrication follows step-A, while to construct the PN-type nanocomposite, the P-type needs to be combined with a second technique, spin-coating, which denoted as step-B. The P-type sample preparation was commenced by drop-casting a small amount of polymer solution onto a glass substrate and was kept for sometimes to dry it in a slow process gradually. Once the dilute polymer layer gets dry, the attached thick polymer layer was soaked into NaOH solution to peel off the polymer layer from the glass substrate.

The thick polymer layer was then put carefully on top of an empty AAO template to be melted for 30 minutes. The AAO template was then injected via melting polymer during the heating process and slowly cooled down in ambient temperature. Finally, the infiltrated AAO template was stuck up-side-down onto a copper tape and submerged within NaOH for 12 hours to dissolve the template, for an etching process, and leave behind the free-standing polymer.

For PN-type nanocomposite fabrication, the construction steps are similar as in the previous P-type production. However, in the PN-type, the second N-type material was infiltrated using a spin coating on top of the P-type. The PN-type etching process follows the same steps as been explained in the previous paragraph. Also, the etching process of an infiltrated AAO template follows the process that was conducted by Azzuliani et al. (Doris, 2017 #347).

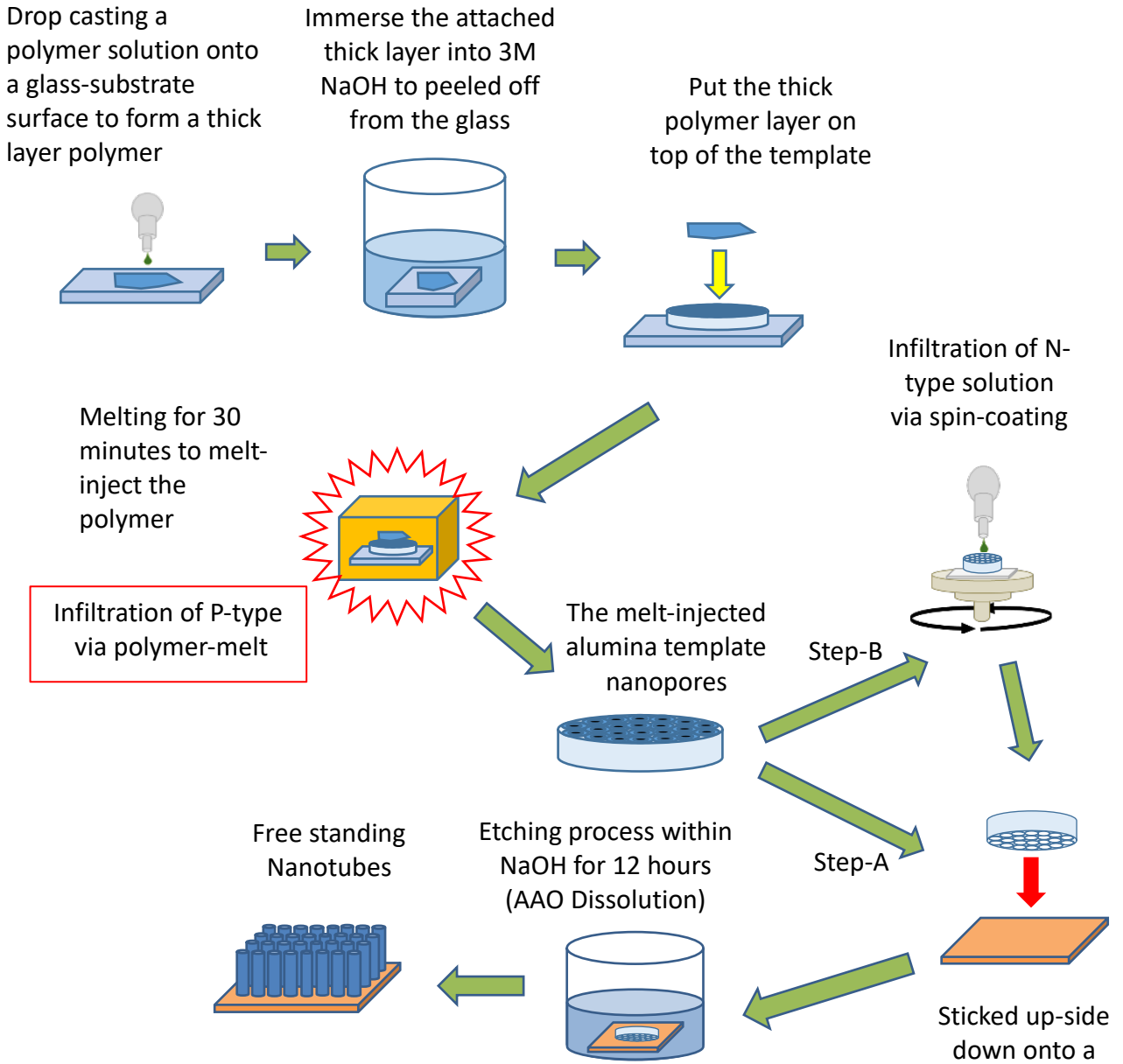


Figure 3: Schematic diagram of the experimental design of the polymer-melt technique to construct P-type nanostructure and PN-type nanocomposite

Sample	Concentration (mg/ml)	Temperature (θ)	Sample label (P-type)	Sample label (PN-type)
1	5	200	PMt-200	PNMt-200
2	5	250	PMt-250	PNMt-250
3	5	300	PMt-300	PNMt-300
4	5	350	PMt-350	PNMt-350
5	5	400	PMt-400	PNMt-400
6	5	450	PMt-450	PNMt-450

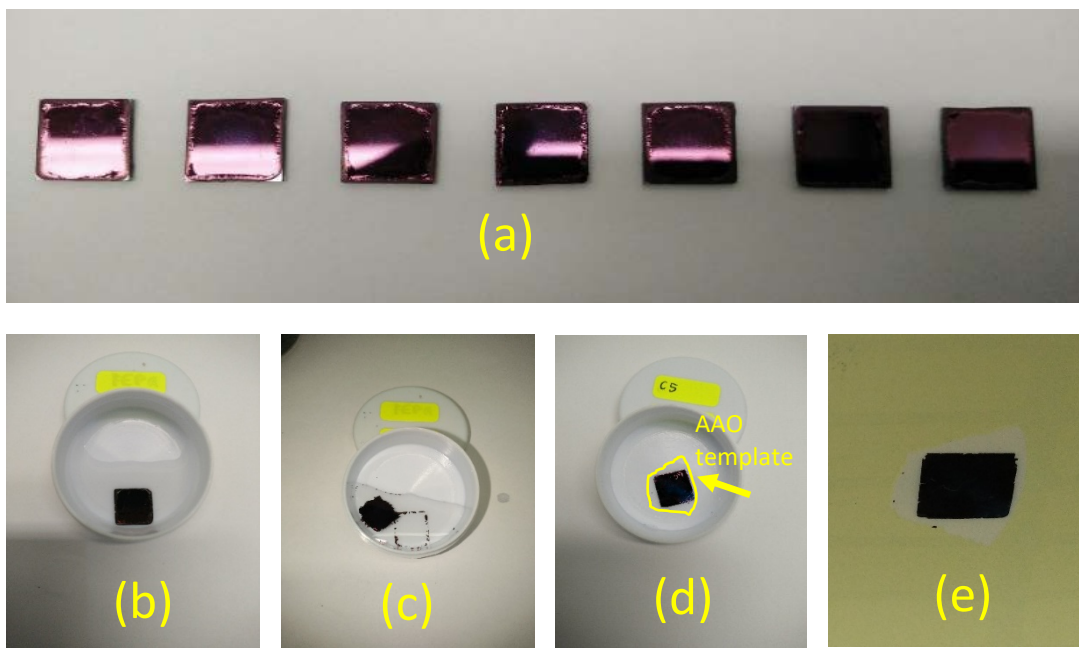


Figure 4 (a) A set of produced PCPDTBT thick layer prior immersion process into NaOH solution to be exfoliated from the glass substrate. Process of peeling off PCPDTBT thick film from a glass substrate (b); Immersion of attached polymer layer within 3 M NaOH (c); A thick polymer layer peeled off from glass surface (d); Thick polymer layer is positioned on top of AAO template after rinsed with D.I water (AAO template is shown as a yellow line), and (e) Thick polymer layer stuck on top of AAO template.

Results and discussions

The previous study that was conducted by Azzuliani et al. has elucidated the results of nanostructures formation which produced based on the mechanical infiltration process via centrifugal force (Doris et al., 2017). In this present investigation, thermal energy is utilized as a driving force to inject prospective material into the AAO nanopores, yet the wetting process still plays an essential role; however, without the involvement of solvent during the infiltration since the solvent is merely used to mix the intended materials to produce a thick layer polymer after the solution solidify by evaporating the solvent. Both mechanical and thermal energy altogether have ever been used to construct nanomaterials, such as nanoballs and nanowires, as what has been done by Kuo et.al in which the melting alloy at high temperature was placed in combination with a high-speed rotation of centrifugal to realize unique nanostructures whereby the AAO nanopores is still used as a primary mold (Kuo & Chao, 2005). Nevertheless, in this thesis, these two combined constructions techniques were separated into two different infiltration mechanisms instead of merging it simultaneously as one technique. Thereby, the effect of the external driving force from each source be able to differentiate and analyzed in its relationship to the properties of the revealed nanomorphology. Figure 4.12 illustrates the infiltration direction of the melt-wetting inside the nanochannel of an AAO template. Some forces that might be involved in the melt-inject process, such as cohesion, adhesion, and the gravitation. The cohesion force (F_{coh}) comes from interaction of molecules inside the melting polymer. The adhesion force (F_{adh}) is the force that exist when the polymer molecules make contact with the AAO nanochannel's wall. The third driving force that may present during the infiltration process is gravity (F_g). A combination of the three forces should control the nanostructures formation process inside the nanochannel other than the melting temperature itself that agitates the molecular interactions

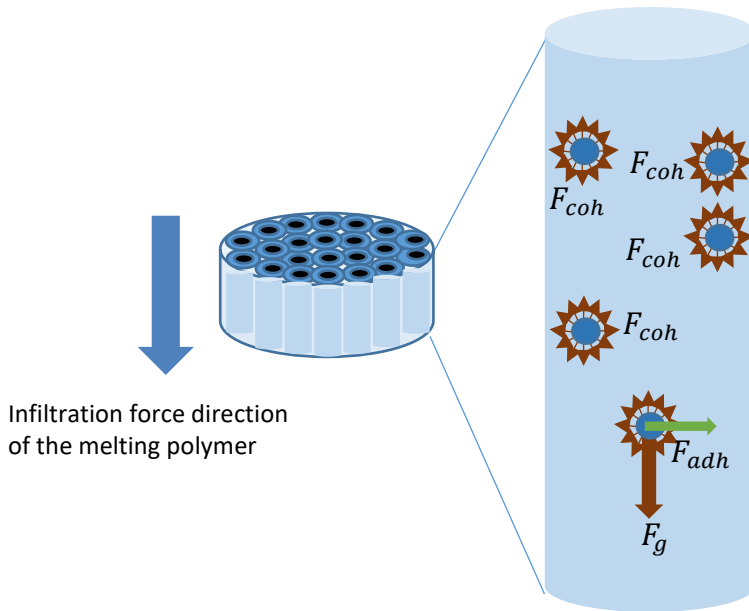
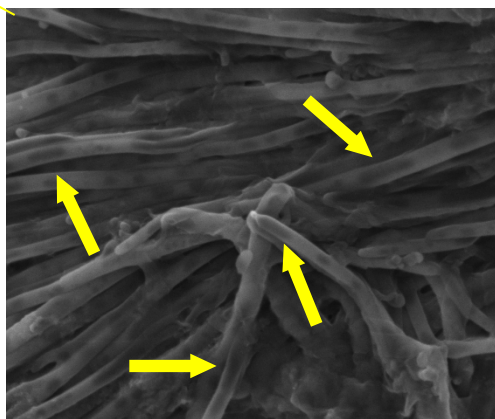
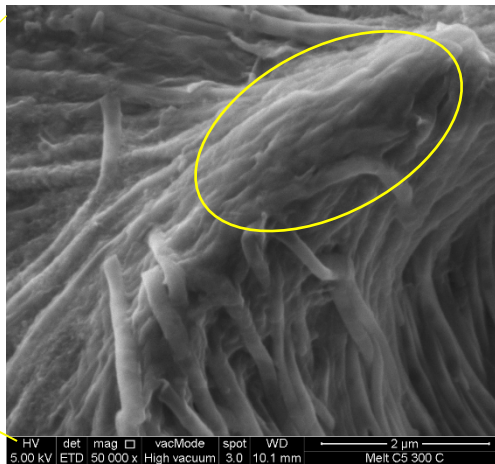
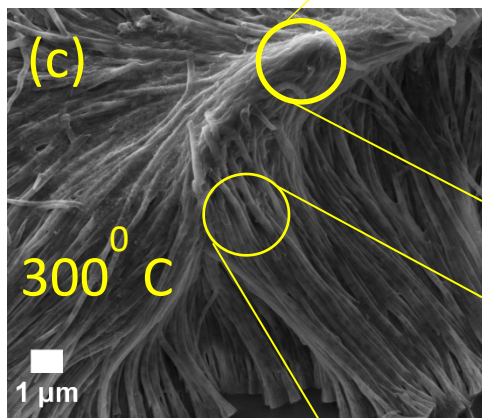
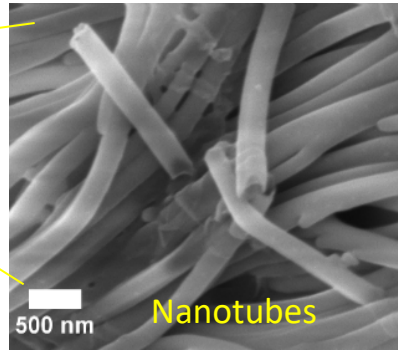
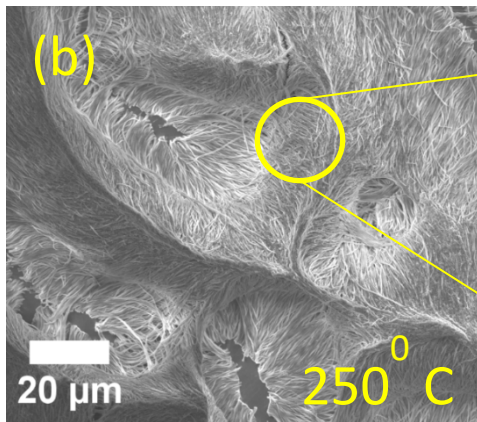
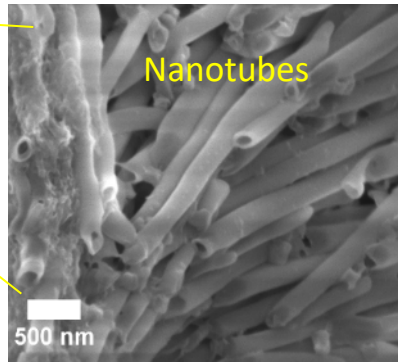
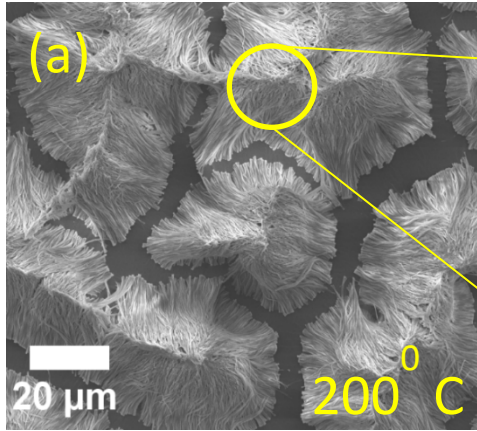


Figure 5: Illustration of polymer melting process inside the nanochannel of the AAO template.

Morphological properties

The constructed polymer nanostructures depend on the wetting condition of the polymer. In a dilute phase, the polymer solution can yield nanotubes whereas prepare it in the melting condition lead to end-result as either nanorods or nanowires (Bordo, Schiek, & Rubahn, 2014). Figure 4.13(a)-(f) exposes PCPDTBT nanostructures construction at various melting temperatures. At 200⁰ C, the melting polymer seems to have filled in the AAO template and the revealed structures are nanowires as exhibited in Figure 4.13 (a) with groups of clusters arrangement and the wide gaps between the clusters. The length of the nanowires, ~20 μm , with an open-end tip that shown in the inset indicates a hollow tube (nanotubes). At 250⁰ C, as can be seen in Figure 4.13(b), the produced structures are quite similar to the previous one, nanowires with an open-end structure (as represented in the inset); nevertheless, its configuration is denser and longer tube, with more than ~40 μm long for every single tail.



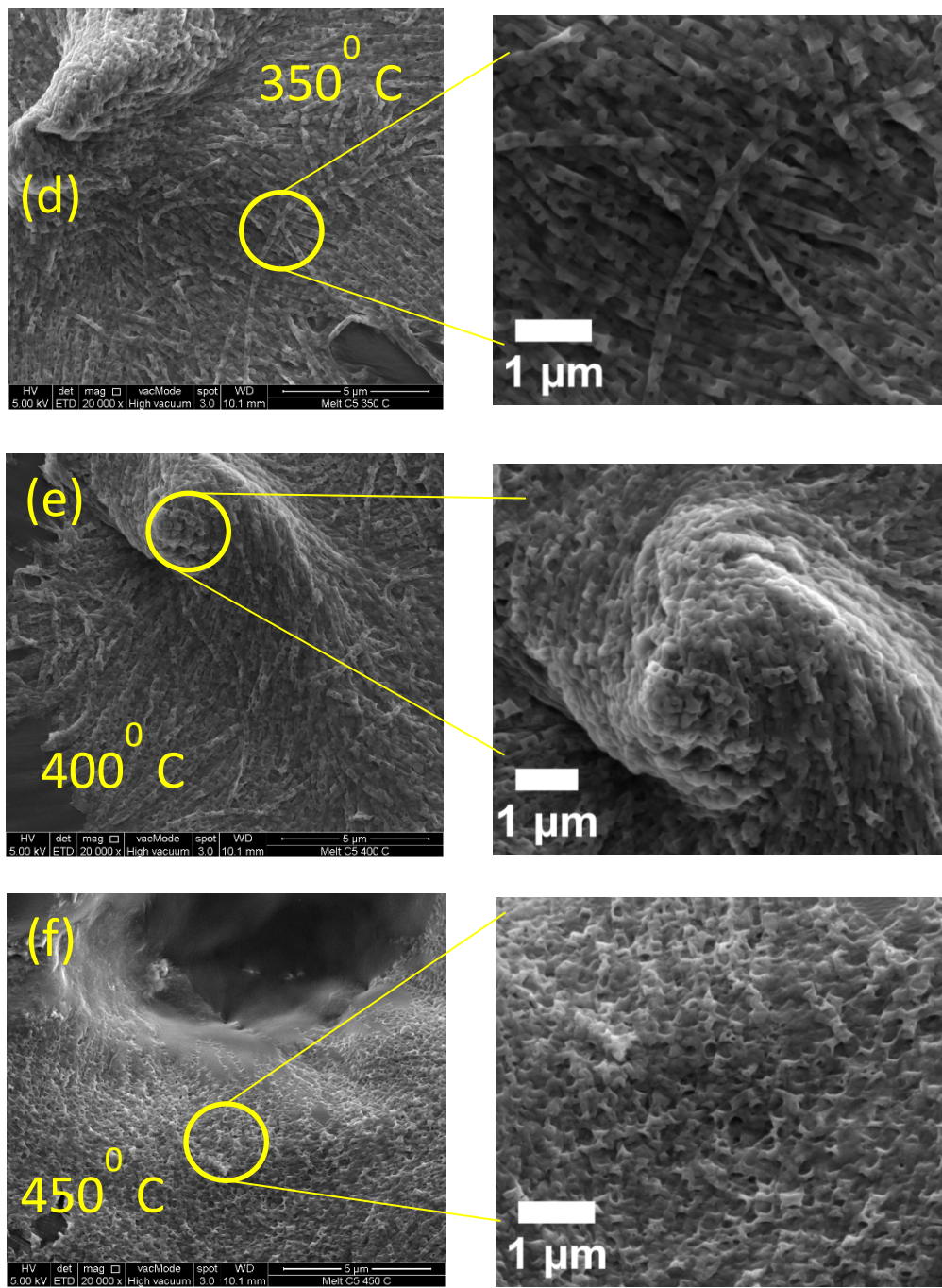


Figure 6: FESEM images of PCPDTBT nanostructures produced at various melting temperatures (200-450⁰ C). (a) PMt-200; (b) PMt-250; (c) PMt-300; (d) PMt-350; (e) PMt-400; (f) PMt-450.

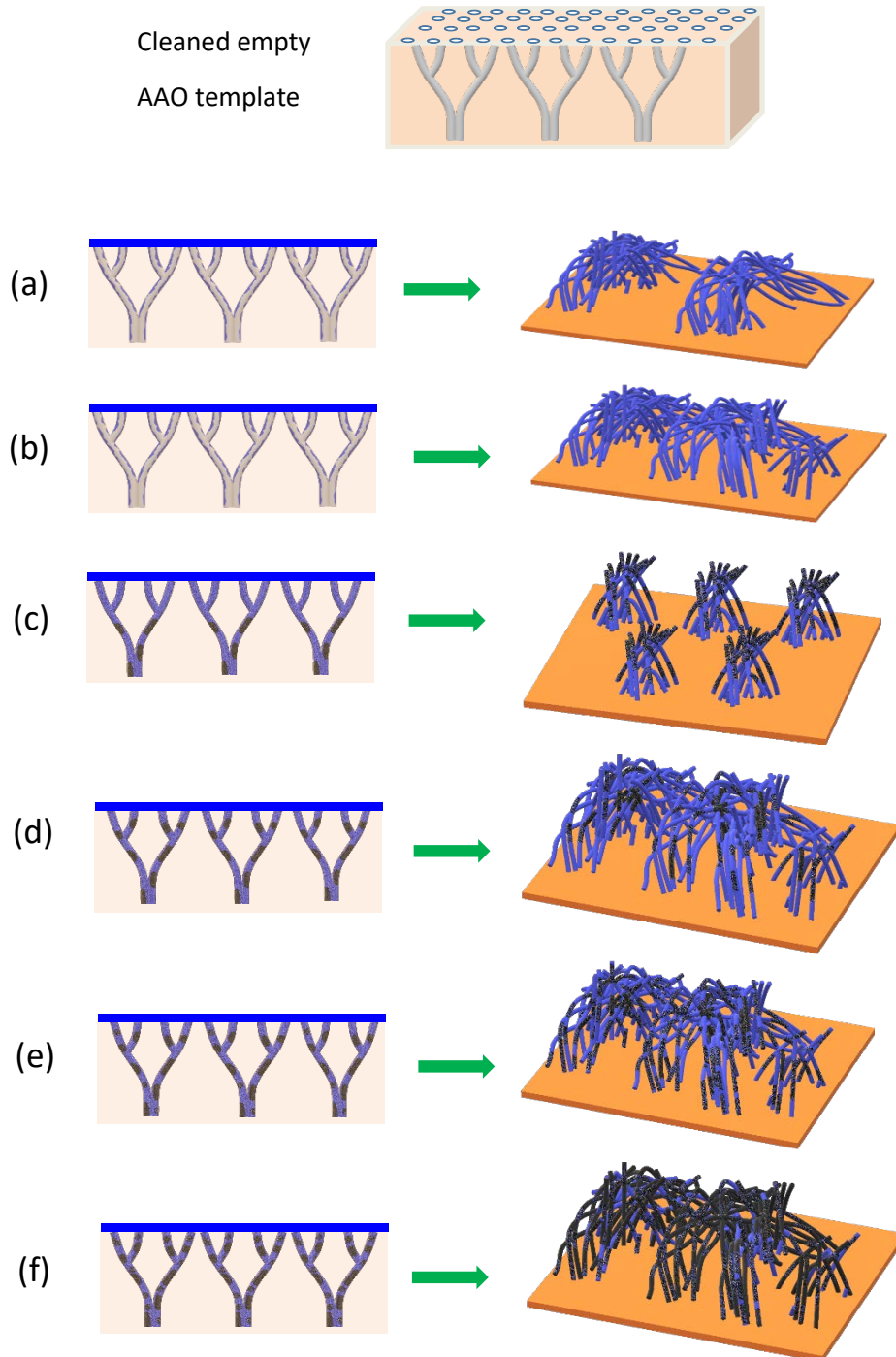


Figure 7: Schematic illustration of the proposed infiltration mechanism in the AAO nanopores via polymer-melt assisted wetting for each of melting temperature (a) PMt-200; (b) PMt-250; (c) PMt-300; (d) PMt-350; (e) PMt-400; and (f) PMt-450⁰ C.

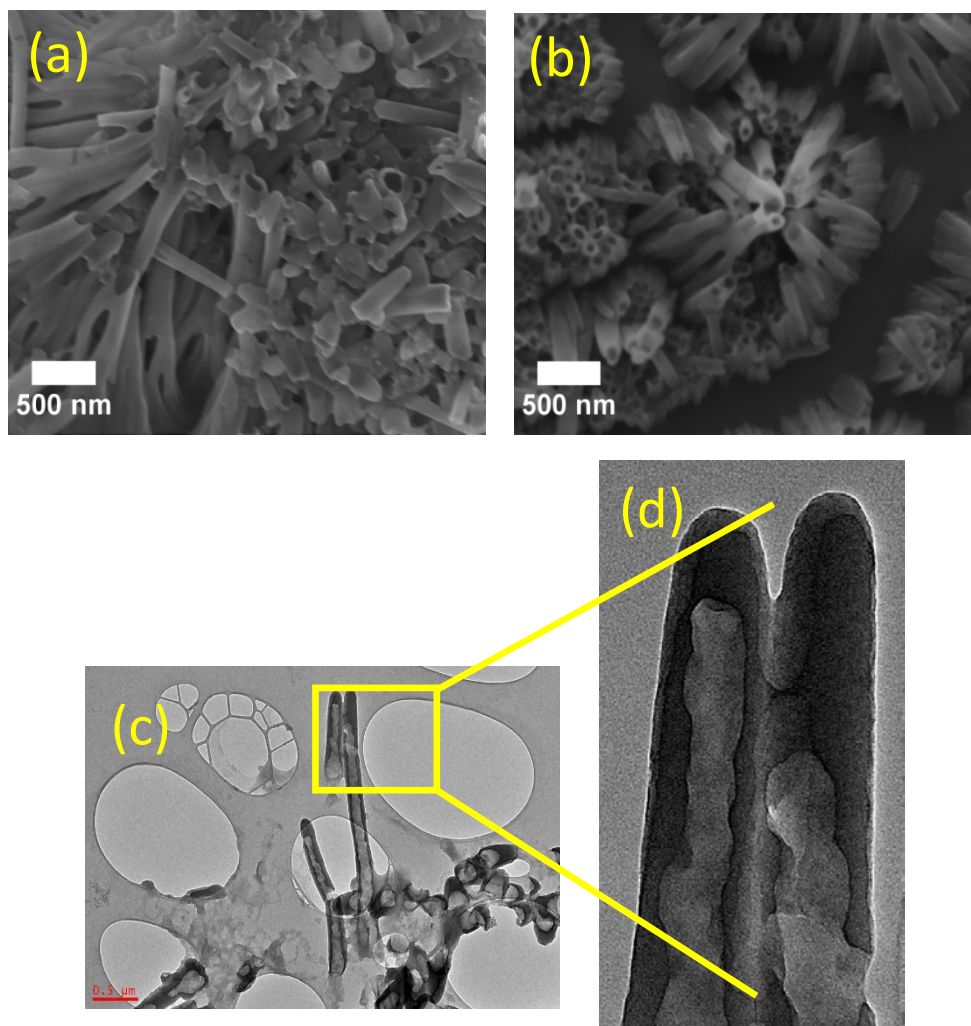


Figure 8 FESEM and TEM results of PCPDTBT:PC71BM to form PN-type nanocomposite. (a) PNMt-200 (b) PNMt-250 (c) TEM image of PNMt-250 and (d) high magnification.

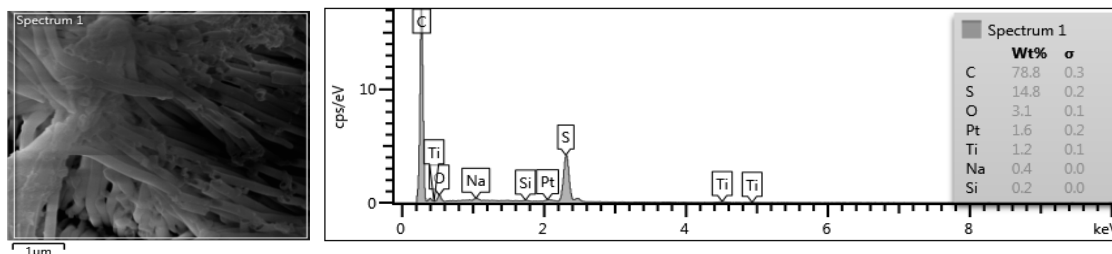


Figure 9xxxxxx

Optical properties

Figure 10 displays the absorption and photoluminescence properties of PCPDTBT nanostructures that were produced at various melting temperatures. Generally, in a solid-state form, the absorption range characteristics of the PCPDTBT is within maxima of 350-450 nm (CPDT) and 500-850 nm (BT) (Mühlbacher et al., 2006; C. Soci et al., 2007). A higher melting temperature has made the absorption range (BT unit) of the some produced nanostructured polymer shifted to the shorter wavelength as shown in Figure 4.15(a) on samples; PMt-300, -350, -400 and -450. On the contrary, the polymer nanostructures that were fabricated at temperatures 200⁰ and 250⁰ C have a BT unit that is still in the range of 500-850 nm (PMt-200 and -250).

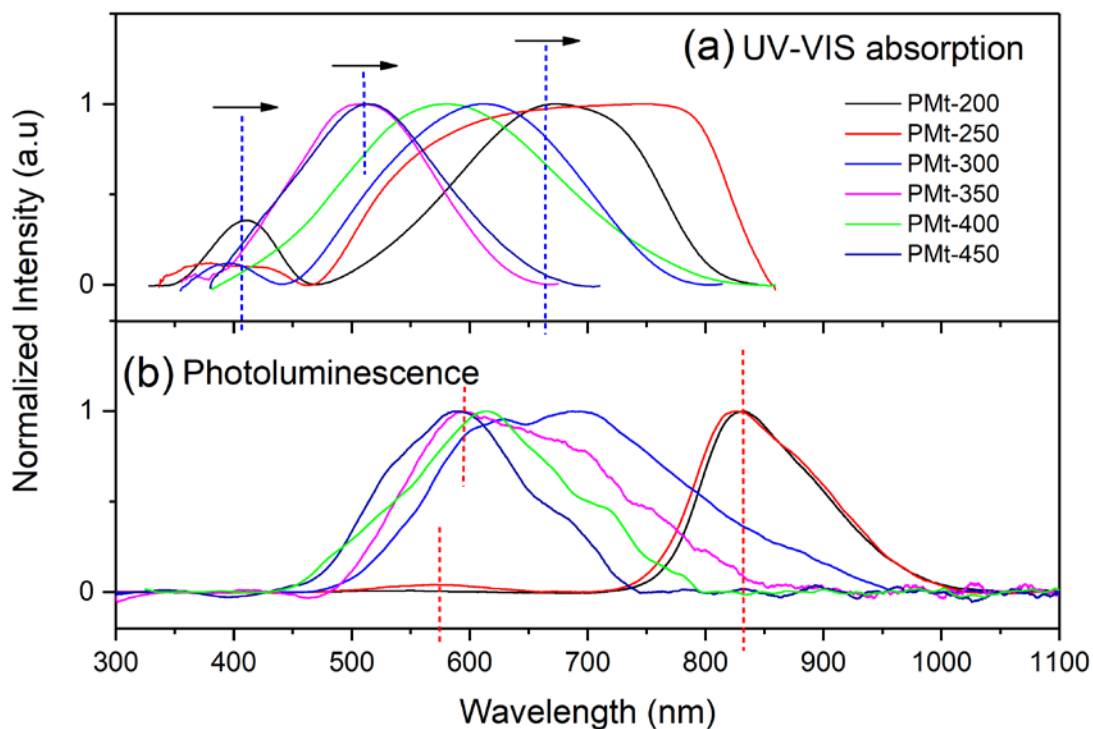


Figure 10: (a) Absorption spectra of the produced PCPDTBT nanostructures at various melting temperature and (b) the respected emission spectra.

It is observed that at temperatures 200°C (PMt-200) and 250°C (PMt-250) respectively are the appropriate melting temperatures for realizing PCPDTBT nanostructures. Increasing the melting temperature has shifted the absorption spectrum (BT) to the shorter wavelength which indicating the decreasing order of the polymer chain (large donor-acceptor twist angle) and conjugation length of the polymer. The disordering polymer chains have suppressed charge transfer between the CPDT and BT units (E. J. J. Martin et al., 2015).

Unarguably, it is seen the order degradation occurs on the PMt-300, PMt-350, PMt-400, and PMt-450. The shifting in the photoluminescence also follows the pattern of peaks shifting in the absorption, Stokes shift, in which the peaks are shifting to lower wavelength as the melting temperature move to a higher value, as displayed in Figure 4.15(b). Demonstrably, the degree of ordering in the polymer follows the melting temperatures that are employed. The ordering of the polymer chain is certainly also reflected in the nanomorphology as shown in the previous FESEM result in Figure 4.13(a-b) on PMt-200 and PMt-250, which observed have flawless structures compared to the other samples.

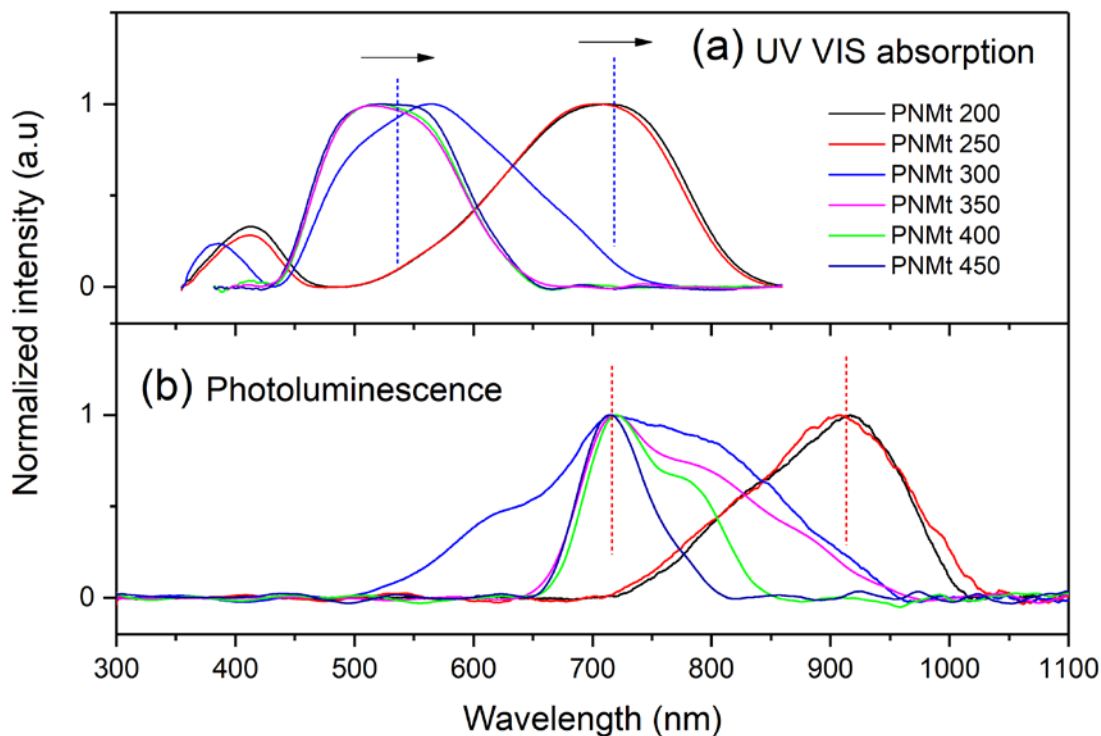
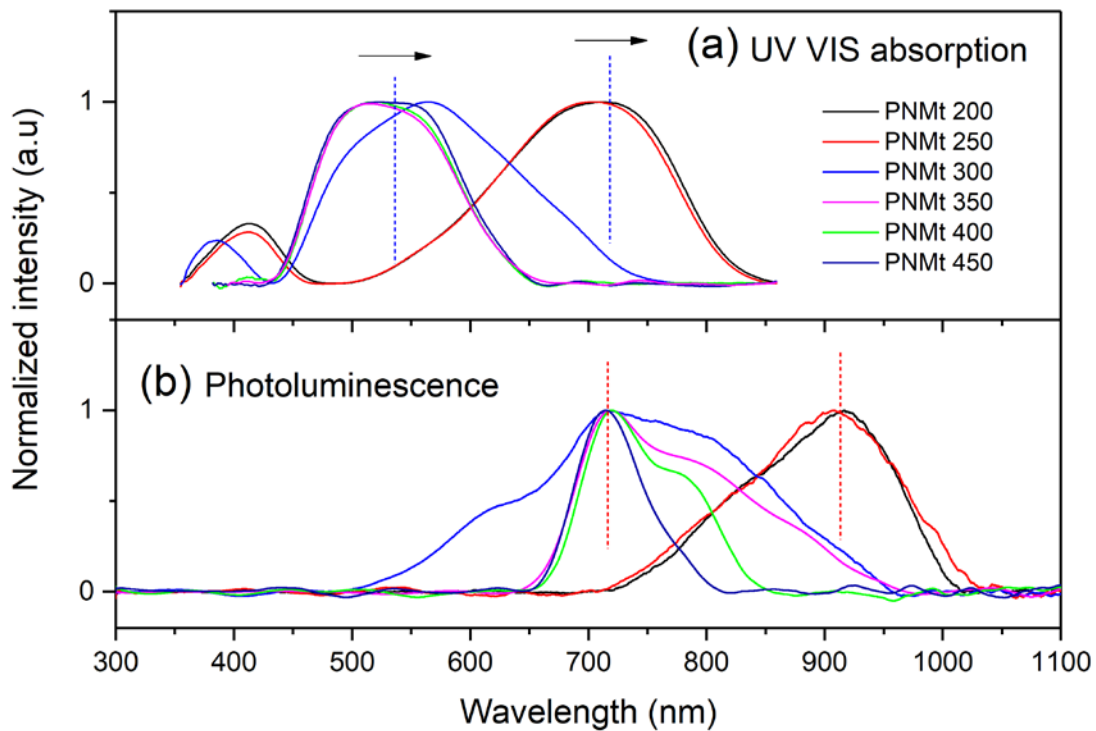


Figure 11: (a) Absorption spectra of the produced PCPDTBT:PC71BM nanocomposite and (b) the respected emission spectra.

Figure 5.10(a)&(b) displays the UV-VIS absorption and the photoluminescence spectra of the PCPDTBT:PC₇₁BM respectively. It is unarguably indicating that there are only two melting temperatures, PNMt-200 and 250, provides exceptional optical response on red-shifted while the rest samples at PNMt-300, 350, 400, and 450, in contrary, are shifting to the blue shift. The revealed optical responses in the PN-type nanocomposite are similar to the previous P-type optical properties which has been investigated in Chapter 4. The BT unit absorption response lies in the range of 500-850 nm. However, the PN-type composites have redder-more shifted, maxima at 720 nm, compared to the P-type as shown in the previous chapter 4 (Figure 4.15) that stretch out in the range of 460-825 with the maxima at 660 nm. That occurs, most probably, introducing the PC₇₁BM into PCPDTBT has increased nanoscale phase segregation inside the PCPDTBT:PC₇₁BM system that might lead to a higher degree of polymer ordering (Peet et al., 2007).



Structural properties

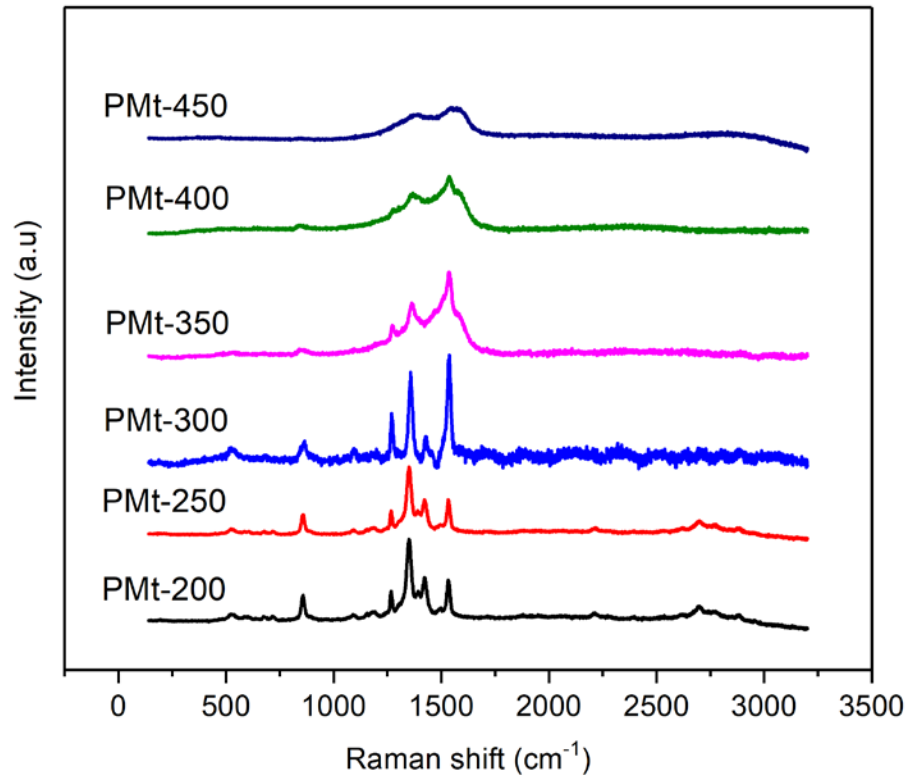


FIGURE: Raman shift measurements of the produced PCPDTBT at various melting temperatures.

TABEL: Raman mode frequencies (cm^{-1}) and the assignments of the P-type PCPDTBT nanostructures.

Peak	PMt-200	PMt-250	PMt-300	PMt-350	PMt-400	PMt-450	Vibrational Assignments
ν_1	523	517	523	-	-	-	Thiophene: Ring deformation
ν_2	675	679	689	-	-	-	Out-of-plane CH deformation vibration
ν_3	714	716	724	-	-	-	Out-of-plane CH deformation vibration
ν_4	858	857	865	841	840	-	Out-of-plane CH_2 deformation vibration
ν_5	1092	1095	1094	-	-	-	CH_3 Rocking vibration
ν_6	1192	1187	1198	-	-	-	CH_3 Rocking vibration
ν_7	1267	1268	1270	1273	1280	-	BT: Symmetric In-plane (CH wag)
ν_8	1349	1350	1357	1363	1366	1384	BT: CH deformation “concert wave” (CH wag) C-H deformation (isopropyl group) CPDT: Thiophene; C=C in-plane vibration
ν_9	1422	1422	1430	-	-	-	CPDT: C-C stretch (Dithiophenes). CPDT: Thiophene; C=C in-plane vibration
ν_{10}	1532	1532	1536	1534	1537	1542	BT: C-C stretch (in-plane CH wag) CPDT: Thiophene; C=C in-plane vibration
ν_{11}	2213	2214	2215	-	-	-	$\text{C}\equiv\text{C}$ stretching vibration
ν_{12}	2691	2697	2699	-	-	-	CH stretching

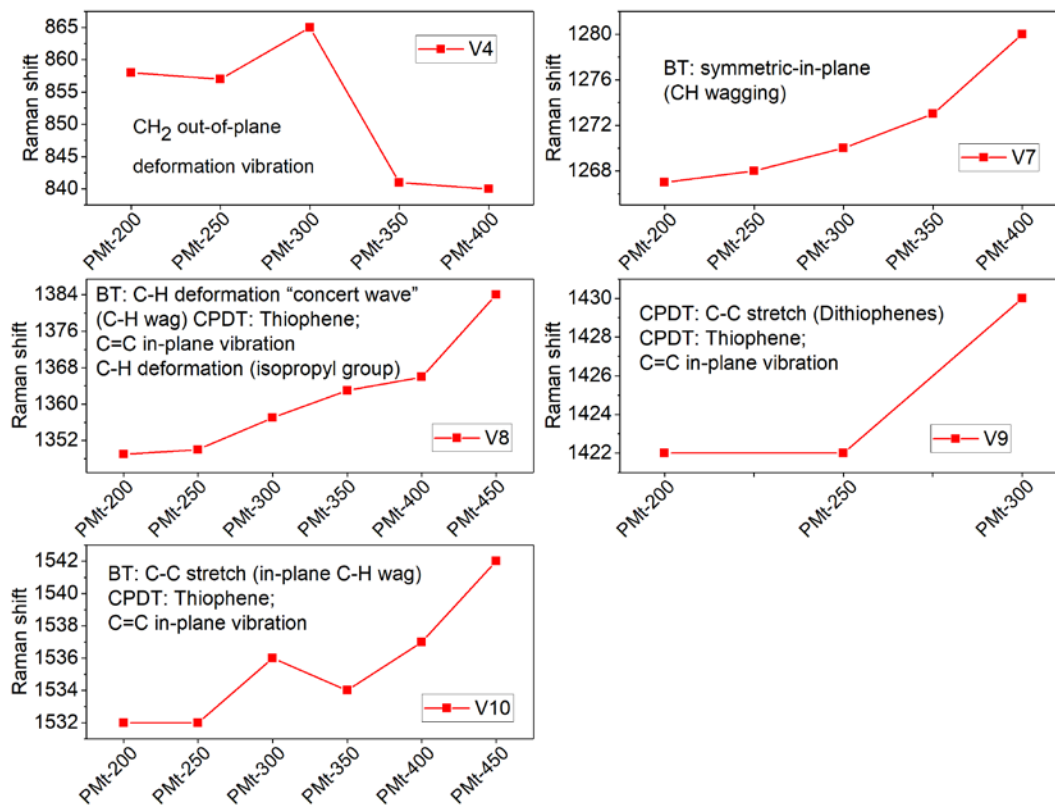


FIGURE: Summary of Raman shiftings on high intensities of the assignments derived from Table

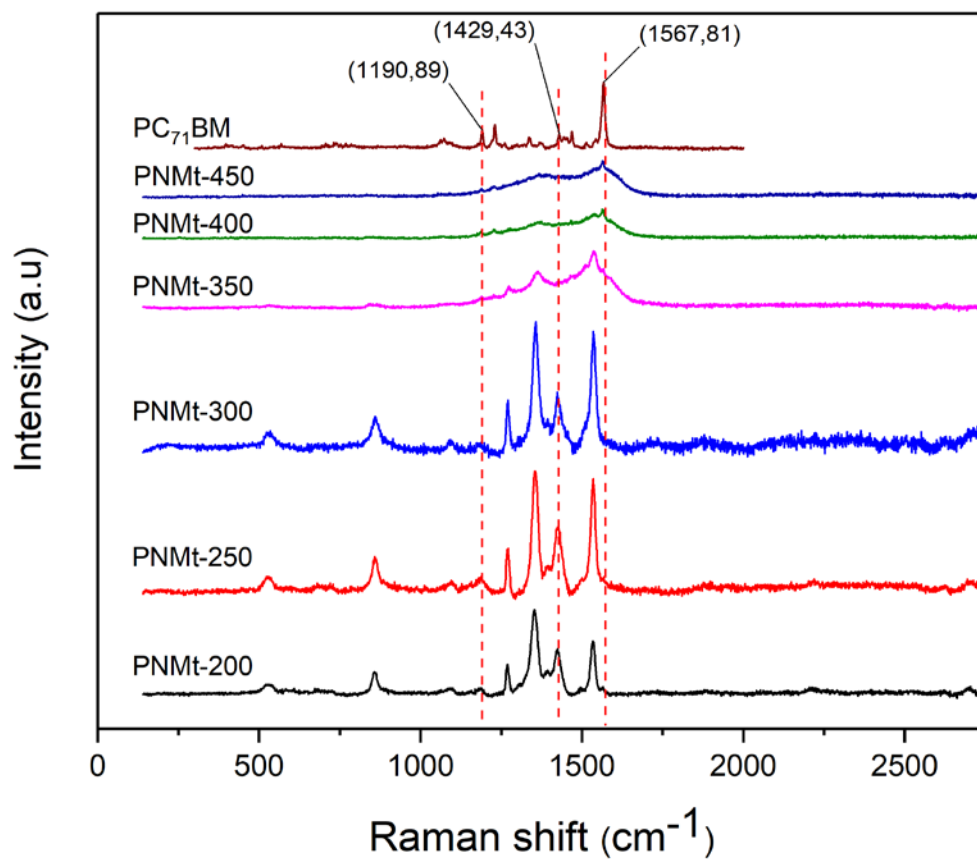


FIGURE: Raman shiftings of constructed PCPDTBT:PC₇₁BM

Raman mode frequencies and assignments (cm^{-1}) of PCPDTBT:PC₇₁BM nanocomposite

Peak	PNMt-200	PNMt-250	PNMt-300	PNMt-350	PNMt-400	PNMt-450	Vibrational Assignments
ν_1	529	528	535	-	-	-	Thiophene: Ring deformation
ν_2	673	680	-	-	-	-	Out-of-plane CH deformation vibration
ν_3	715	720	-	-	-	-	Out-of-plane CH deformation vibration
ν_4	857	858	859	845	-	-	Out-of-plane CH ₂ deformation vibration
ν_5	1088	1095	1092	1190	1187	1189	CH ₃ Rocking vibration
ν_6	1187	1187	1187	1227	1226	1227	CH ₃ Rocking vibration
ν_7	1269	1271	1270	1274	1279	-	BT: CH deformation (Symmetric In-plane)
ν_8	1352	1355	1357	1364	1374	1372	BT: CH deformation "concert wave" (CH wag) CPDT: Thiophene; C=C in-plane vibration & C-H deformation (isopropyl group)
ν_9	1424	1423	1423	-	-	-	CPDT: C-C stretch (Dithiophenes). CPDT: Thiophene; C=C in-plane vibration
ν_{10}	1533	1534	1536	1536	1563	1564	BT: C-C stretch (in-plane C-H wag) CPDT: Thiophene; C=C in-plane vibration
ν_{11}	2213	2220	2224	-	-	-	C≡C stretching vibration
ν_{12}	2703	2694	2696	-	-	-	CH stretching

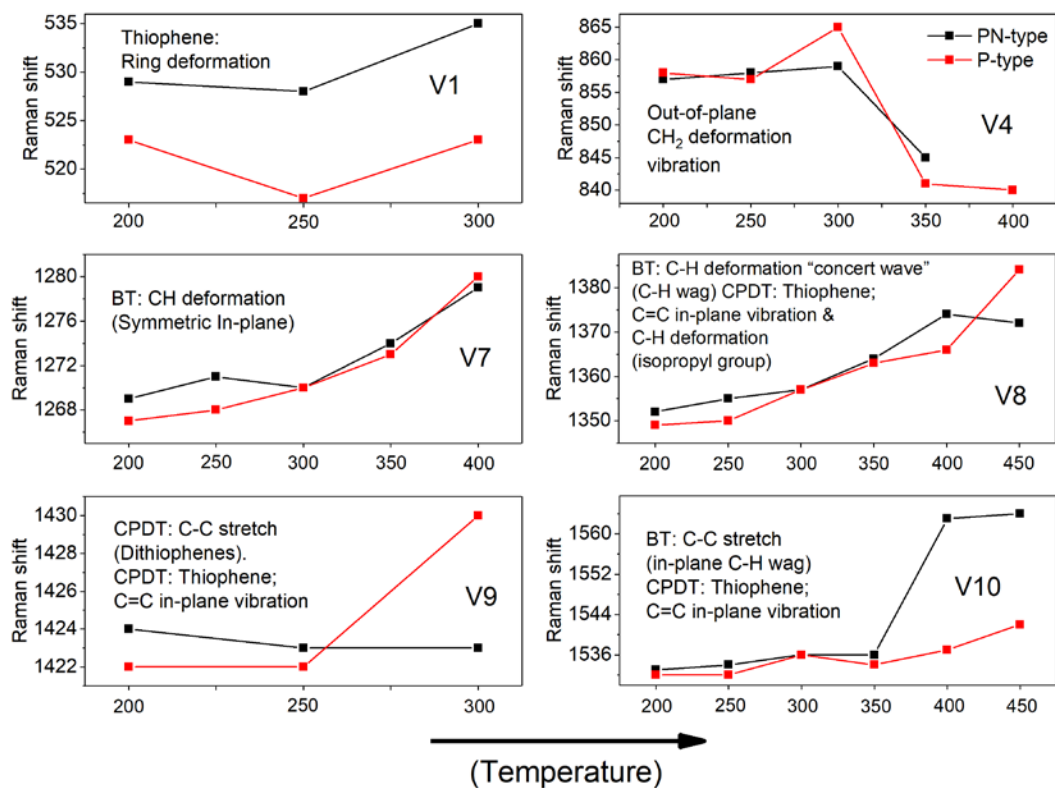


FIGURE: Summary of the Raman shifting on each of assignment based on particular high intensities derived from Table 4.2 (P-type) and Table 5.2 (PN-type).

Conclusion

Polymer melt wetting process (Ali et al., 2015)

Wetting (Zhang et al., 2006)

There are some ways that have been applied to fabricate nanostructures by using alumina template nanopores through the wetting process either melt wetting or solution wetting. An external forces have been applied whilst a wetting process takes place. For instance, fabrication of a polymer nanostructures using melt wetting method as applying a vibration could enhance the infiltration process into the nanopores (Xie, Xu, & Yung, 2012) (Kong, Xu, Yung, Xie, & He, 2009). **the surface tension and viscosity of the liquid, the size of the capillary, and the length of the channel determine the rate of liquid flow in capillary** $dz=dt \frac{1}{4} Rg \cos \gamma c=0.4ZzP$ (Kim, Xia, & Whitesides, 1995). **The viscosity of the polymer melts usually decreased with the increase of temperature. Hydrodynamics model in slit shape nanochannel (Bhadoria & Aluru, 2013)**

REFERENCES

- Ali, S., Tian, W., Ali, N., Shi, L., Kong, J., & Ali, N. (2015). Polymer melt flow through nanochannels: From theory and fabrication to application. *RSC Advances*, 5(10), 7160-7172. doi:10.1039/C4RA14787A
- Bhadoria, R., & Aluru, N. R. (2013). A quasi-continuum hydrodynamic model for slit shaped nanochannel flow. *The Journal of Chemical Physics*, 139(7), 074109. doi:doi:<http://dx.doi.org/10.1063/1.4818165>
- Bordo, K., Schiek, M., & Rubahn, H.-G. (2014). Nanowires and nanotubes from π -conjugated organic materials fabricated by template wetting. *Applied Physics A*, 114(4), 1067-1074. doi:10.1007/s00339-014-8226-5
- Doris, M., Aziz, F., Alhummiyany, H., Bawazeer, T., Alsenany, N., Mahmoud, A., . . . Supangat, A. (2017). Determining the effect of centrifugal force on the desired growth and properties of pcpdtbt as p-type nanowires. *Nanoscale Research Letters*, 12(1), 67. doi:10.1186/s11671-017-1851-0
- Kim, E., Xia, Y., & Whitesides, G. M. (1995). Polymer microstructures formed by moulding in capillaries. *Nature*, 376(6541), 581-584.
- Kong, J., Xu, Y., Yung, K.-L., Xie, Y., & He, L. (2009). Enhanced polymer melts flow through nanoscale channels under vibration. *The Journal of Physical Chemistry C*, 113(2), 624-629. doi:10.1021/jp809164k
- Kuo, C.-G., & Chao, C.-G. (2005). Fabrication of isolated alloy nanoballs and nanowires using centrifugal force. *Jpn J Appl Phys*, 44(2), 1155-1159. doi:10.1143/JJAP.44.1155
- Xie, Y.-C., Xu, Y., & Yung, K.-L. (2012). Wetting behaviors of hyperbranched polymer composites within ordered porous template under vibration. *Polymer Engineering & Science*, 52(1), 205-210. doi:10.1002/pen.22068
- Zhang, M., Dobriyal, P., Chen, J.-T., Russell, T. P., Olmo, J., & Merry, A. (2006). Wetting transition in cylindrical alumina nanopores with polymer melts. *Nano letters*, 6(5), 1075-1079. doi:10.1021/nl060407n

